AD NUMBER

AD483324

NEW LIMITATION CHANGE

TO

Approved for public release, distribution unlimited

FROM

Distribution authorized to U.S. Gov't. agencies only; Administrative/Operational Use; MAY 1966. Other requests shall be referred to Commanding General, U.S. Army Electronics Command, Attn: AMSEL-KL-EM, Fort Monmouth, NJ 07703-5601.

AUTHORITY

USAEC ltr, 9 Feb 1972

Report No. 8
Final Report

Covering the Period
1 June 1965 to 31 December 1965

Investigation of MICROWAVE DIELECTRIC-RESONATOR FILTERS

Prepared for:
U. S. ARMY ELECTRONICS COMMAND
FORT MONMOUTH, NEW JERSEY

CONTRACT NO. DA-36-039-AMC-02267(E)
TASK NO. IP6 22001 A 057 02

By: S. B. Cohn and E. N. Torgow

DISTRIBUTION STATEMENT

Each transmittal of this document outside the Department of Defense must have prior approval of CG, U. S. Army Electronics Command, Fort Monmouth, N. J. Attn: AMSEL-KL-EM

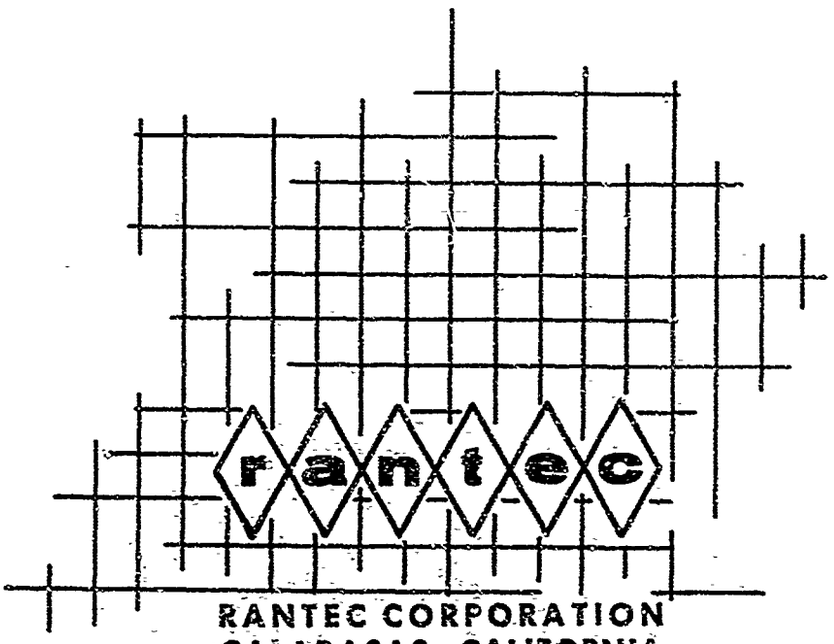

RANTEC CORPORATION
CALABASAS, CALIFORNIA

NOTICES

Disclaimers

The findings in this report are not to be construed as an official Department of the Army position, unless so designated by other authorized documents.

The citation of trade names and names of manufacturers in this report is not to be construed as official Government indorsement or approval of commercial products or services referenced herein.

Disposition

Destroy this report when it is no longer needed. Do not return it to the originator.

Report No. 8

Final Report

Covering the Period
1 June 1965 to 31 December 1965

Investigation of MICROWAVE DIELECTRIC-RESONATOR FILTERS

Prepared for:
U. S. ARMY ELECTRONICS COMMAND
FORT MONMOUTH, NEW JERSEY

CONTRACT NO. DA-36-039-AMC-02267(E)
TASK NO. 1P6 22001 A 057 02

By: S. B. Cohn and E. N. Torgow

Rantec Project No. 31625

Approved:

Seymour B. Cohn

SEYMOUR B. COHN, Technical Director

TABLE OF CONTENTS

TABLE OF CONTENTS (Cont'd)

LIST OF ILLUSTRATIONS

LIST OF ILLUSTRATIONS (Cont'd)

LIST OF TABLES

SECTION I

PURPOSE

This program is intended to study the feasibility of high-dielectric-constant materials as resonators in microwave filters, and to obtain design information for such filters. Resonator materials shall be selected that have loss tangents capable of yielding unloaded Q values comparable to that of waveguide cavities. The materials shall have dielectric constants of at least 75 in order that substantial size reductions can be achieved compared to the dimensions of waveguide filters having the same electrical performance.

SECTION II

ABSTRACT

This report is the last of a series of eight reports on an investigation of microwave dielectric-resonator filters. The accomplishments of the investigation are itemized and discussed, showing that feasibility has been established and design criteria obtained for various configurations of band-pass, band-stop, directional, and diplexer filters containing high-Q, miniature dielectric resonators. The problem of compensating for temperature sensitivity, which has been outside of the scope of this investigation, remains to be solved before applications will be practical. Several approaches to this problem are discussed.

Coupling between dielectric-disk resonators axially oriented along the center line of a cut-off circular tube is analyzed, and a formula for coupling coefficient is derived. A comparison is made between experimental points and the theoretical curve for a pair of disks whose spacing is varied over a wide range. The measured points lie about 14% above the curve, which is reasonable agreement considering the extreme steepness of the curve. For most practical purposes, the accuracy is sufficient and may be improved, if desired, by minor adjustment.

The case of a band-stop dielectric-disk resonator coupled to the magnetic field of a propagating strip line is treated theoretically. A formula for the external Q, Q_{ex}, is derived.

Response curves are given for three waveguide directional-filter configurations utilizing dielectric resonators. In all cases, directional-filter behavior was verified. One configuration used a pair of single-mode disks, the second used one dual-mode disk, and

the third used two dual-mode disks. This third case was by far the most difficult to adjust. Several strip- and slab-line directional filter circuits containing dielectric resonators are discussed, and one of these cases is analyzed.

External loading of the end resonators of a multiple-disk band-pass filter is studied in the case of a parallel-plane boundary. Formulas are given that relate Q_{ex} of a band-pass disk loaded by a short-circuited or open-circuited strip or slab line to the Q_{ex} formulas for the related band-stop propagating-line geometries.

Various techniques are described for joining band-pass and band-stop filters to form three-port diplexers. Approaches are discussed for achieving well matched channel bands when these bands are widely spaced, and when they are closely spaced.

The problems of achieving satisfactory end coupling in the case of a band-pass axially oriented disk geometry are discussed in terms of measured data and theoretical limitations. It is concluded that axial orientation in a cut-off square or circular tube has several practical disadvantages compared to transverse orientation.

SECTION III

CONFERENCES AND PUBLICATIONS

A conference was held at Rantec Corporation on 27-28 July 1965. Mr. E. Mariani of the U. S. Army Electronics Laboratories and Dr. S. B. Cohn and Mr. E. N. Torgow of Rantec Corporation were present. Plans for the final period of the investigation were discussed.

A conference was held on 17 November 1965 at U. S. Army Electronics Laboratories, Fort Monmouth, New Jersey. Those attending were Messrs. J. Agrios, E. Mariani, and N. Lipetz of the Laboratories, and Dr. S. B. Cohn and Mr. E. N. Torgow of Rantec Corporation. The work in progress was discussed and the goals and accomplishments of the entire program were reviewed. Decisions were made concerning the research to be completed and the experimental filters to be delivered.

A paper entitled "Microwave Measurement of High-Dielectric-Constant Materials" has been prepared by Dr. S. B. Cohn and Mr. K. C. Kelly, and has been accepted for publication by IEEE Trans. on Microwave Theory and Techniques.

SECTION IV

FACTUAL DATA

1. Introduction

This Final Report follows a series of seven quarterly reports[1-7] on an investigation of dielectric resonators and their application to microwave filters. The basic principles and characteristics of dielectric resonators are discussed in the First Quarterly Report.[1] The introduction to that report should be consulted for background information, references to earlier work,[8-10] and for a discussion of problems to be solved before dielectric resonators can be used in practice.

The seven preceding reports[1-7] and this current report contain theoretical and experimental studies of a large variety of topics relating to the practical design of band-pass, band-stop, directional, and diplexer filters containing dielectric resonators. These subjects are listed in a logical order in Table 1-1, with references to the reports in which they are treated. The scope and accomplishments of the program are revealed by examination of this table.

The investigation now completed has proven the feasibility of dielectric resonators in many types of filters. The anticipated advantage of high Q (on the order of 10,000) in a volume small compared to that of conventional resonators has been verified. Theoretical and experimental techniques of achieving the couplings needed in filter design have been developed for a large number of useful geometries. Experimental examples of band-pass, band-stop, and directional filters have been given.

One important problem remains to be solved before extensive practical utilization of dielectric resonators in filters can be made.

This is the problem of temperature sensitivity, which has been outside the scope of the investigation now concluded. A titanium-dioxide resonator, for example, exhibits a relative change in dielectric constant of about 1 $(10)^{-3}/^{\circ}C$. The resulting center-frequency change is 0.5 $(10)^{-3}/^{\circ}C$. At 3000 Mc, a $\pm 20^{\circ}C$ temperature variation will affect the center frequency by about ±30 Mc, which cannot be tolerated in most applications. Further investigation to devise methods of reducing temperature sensitivity is therefore necessary. Possible approaches are improvement in materials, temperature regulation, and compensation through proximity of other elements offering the opposite change with temperature.

This Final Report treats a number of technical subjects that round out the work of the complete program. Included are an analysis of axially oriented dielectric disks in circular tubes, an analysis of a band-stop disk coupled to a strip line, further investigation of directional filters, band-pass filters in strip or slab line, diplexer filters, and a discussion of end coupling in the axial-orientation band-pass case.

Table 1-1

SUMMARY OF INVESTIGATION OF DIELECTRIC-RESONATOR FILTERS

Topic	Report and Sub-section Numbers*
A. Properties of Dielectric Disk Resonators	
(1) Analysis of f_o and field distribution	1(2)
(2) Data on f_o including effect of nearby walls	1(2), 3(4), 6(2), 7(5)
(3) Experimental study of first three resonant modes in dielectric cylinder	7(4)
(4) Measurement of Q_u and effect of nearby walls	1(3), 3(4), 5(5), 6(2), 6(4), 7(5)

Table 1-1 (Cont'd)

Topic	Report and Sub-section Numbers*
(5) Methods of ϵ_r measurement, ϵ_r data, and effect of temperature	2(2), 3(3), 5(5), 6(4)
(6) Magnetic dipole moment, stored energy, and intrinsic factor $F = \mu_o m_1^2 / 2W_{m1}$	2(3)
B. Band-Pass Filters	
(1) Approximate equivalence of dielectric resonator to a magnetic dipole	1(1), 2(3)
(2) Generalized theory of coupling between dielectric resonators	2(3)
(3) Coupling coefficient - transverse orientation of disks spaced along a rectangular waveguide below cutoff	2(3,4), 3(2)
(4) Coupling coefficient - axial orientation of disks, rectangular waveguide below cutoff	4(2, 3)
(5) Coupling coefficient - axial orientation of disks, circular waveguide below cutoff	8(2)
(6) End coupling - transverse orientation of disks	4(4)
(7) End coupling - axial orientation of disks	8(7)
(8) End coupling - strip and slab line	8(5)
(9) Experimental band-pass filters	3(5), 4(4)
C. Band-Stop Filters	
(1) General case of dielectric resonator in the field of a propagating TEM line	5(3)
(2) Analysis of dielectric disk in a coaxial line	5(3)
(3) Analysis of dielectric disk in a slab line	5(3)

Table 1-1 (Cont'd)

Topic	Report and Sub-section Numbers*
(4) Analysis of dielectric disk in a strip line	8(3)
(5) Analysis of dielectric disk in a waveguide above cutoff	7(2)
(6) Design of multi-resonator band-stop filters	5(4), 7(2)
(7) Experimental band-stop filters	5(4), 6(3), 7(2)
D. Directional Filters	
(1) Basic properties of directional filters	7(3)
(2) Waveguide directional filters using single- and dual-mode disks	7(3)
(3) Strip- and slab-line directional filters using single- and dual-mode disks	8(4)
(4) Experimental directional filters	8(4)
E. Diplexer Filters	
(1) Basic techniques	8(6)
(2) Design of strip- and slab-line diplexers using dielectric resonators	8(6)

*First number applies to report, second number to Factual Data sub-sections; e.g., 3(4) indicates Third Quarterly Report, sub-section 4.

2. Coupling Coefficient - Axial Orientation in Circular Tube

a. Relation to Previous Analyses

In the Fourth Quarterly Report[4] the case of dielectric-disk resonators oriented axially in cut-off square and rectangular waveguide was analyzed, and a formula for the coupling coefficient between adjacent disks was derived. A graph given in that report comparing measured points and theoretical curves showed excellent

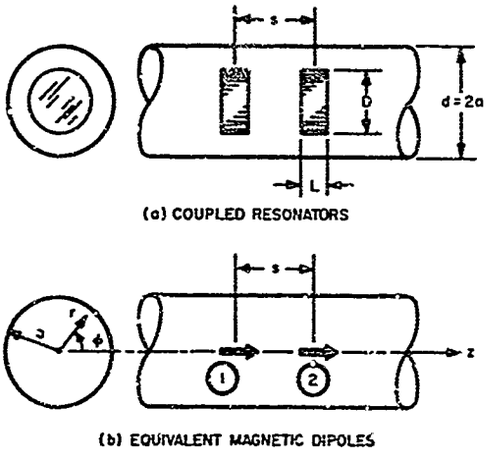

Figure 2-1. Axially-Oriented Dielectric Resonators in a Circular Tube

agreement over a wide range of spacing for a pair of disks in two different sizes of square waveguide. The analysis will now be extended to the case of axial orientation of disks in cut-off circular tubes or waveguides, as shown in Figure 2-1. A comparison of theoretical coupling coefficient with measured data will then be given.

The analysis will be similar to that in the Fourth Quarterly Report for axial orientation in a rectangular waveguide, and will also be similar to that in the Second and Third Quarterly Reports for transverse orientation in a rectangular waveguide. These reports should be referred to for further details on the method of analysis and basic relations.

b. Basic Relationships

As in the case of axial orientation in a rectangular waveguide, the following formula gives the coupling coefficient between a pair of identical resonant magnetic dipoles aligned along the axis of a cut-off circular tube:

$$k = -F \frac{H_{2z}}{m_1} \qquad (2\text{-}1)$$

where m_1 is the magnetic dipole moment of the first dipole and H_{2z} is the axial component of magnetic field at the second dipole due to the

first dipole. The constant F is a function only of the geometry of the dielectric-disk resonator and its ϵ_r value. The following simple formula for F is derived in the Second Quarterly Report, where also a more exact but complex formula is given:

$$F = \frac{\mu_o m_1^2}{2W_{m1}} = \frac{0.927 D^4 L \epsilon_r}{\lambda_o^2}, \quad 0.25 \leq L/D \leq 0.7 \tag{2-2}$$

In the above equations and in the following discussion, the dielectric disk (L<D) is assumed to be in its lowest-order mode of resonance, in which case the external field of the disk resembles that of a magnetic dipole directed along the axis of the disk. Since $H_z = 0$ for TM modes, only TE modes need be considered.

Utilizing the notation and basic relations given in the Second and Fourth Quarterly Reports, we obtain the following equation for H_{2z} as a summation of the contributions of all TE_{mn} modes excited by the axial dipoles.

$$H_{2z} = \sum_{m,n} a_{mn} h_{zmn} e^{-\alpha_{mn} s} \tag{2-3}$$

where the factors a_{mn} are coefficients that will be evaluated below, the axial magnetic-field components h_{zmn} are normalized functions of the transverse co-ordinates r and ϕ, α_{mn} are attenuation constants of the cut-off mode, and s is the center-to-center spacing of the dipoles. The magnetic-field normalization is achieved by imposing the following relation on the transverse-plane component h_{tmn}:

$$Z_{o_{mn}} \iint h_{tmn}^2 \, dS = 1 \tag{2-4}$$

where

$$h_{tmn}^2 = h_{rmn}^2 + h_{\phi mn}^2 \tag{2-5}$$

and

$$Z_{o_{mn}} = \frac{j2\pi\eta}{\alpha_{mn}\lambda} \tag{2-6}$$

The field functions h_{zmn}, h_{rmn}, and $h_{\phi mn}$ are as follows for the TE_{mn} mode:[11]

$$h_{zmn} = C_{mn} J_m(k_{cmn} r) \cos m\phi \tag{2-7}$$

$$h_{rmn} = -\frac{\alpha_{mn} C_{mn}}{k_{cmn}} J'_m(k_{cmn} r) \cos m\phi \tag{2-8}$$

$$h_{\phi mn} = \frac{m\alpha_{mn} C_{mn}}{r k_{cmn}^2} J_m(k_{cmn} r) \sin m\phi \tag{2-9}$$

where $J_m(u)$ is the Bessel function of the mth order and first kind, $J'_m(u) = dJ_m(u)/du$, and

$$k_{cmn} = 2\pi/\lambda_c = u_{mn}/a \tag{2-10}$$

is the cut-off wave number, u_{mn} being the nth root of

$$J'_m(u_{mn}) = 0 \tag{2-11}$$

The constant C_{mn} is evaluated for each mode such that the normalization relation Eq. 2-4 is satisfied.

c. Normalization of Magnetic Field Components

The constant C_{mn} in Eqs. 2-7 through 2-9 will now be determined by means of the normalization relationship, Eq. 2-4. Thus

$$I = Z_{omn} \iint \left(h_{\phi mn}^2 + h_{rmn}^2 \right) dS = 1 \tag{2-12}$$

Let

$$I_1 = Z_{omn} \iint h_{\phi mn}^2 \, dS$$

$$= \frac{m^2 \alpha_{mn}^2 Z_{omn} C_{mn}^2}{k_{cmn}^2} \int_0^{2\pi} \int_0^a \left(\frac{J_m(k_{cmn} r)}{k_{cmn} r} \right)^2 \left(\sin^2 m\phi \right) r \, dr \, d\phi \tag{2-13}$$

The possible values of m and n in the case of a TE_{mn} mode in circular waveguide are $m \geq 0$ and $n \geq 1$. Therefore,

$$\int_0^{2\pi} \sin^2 m\phi \, d\phi = \pi \qquad \text{for } m \geq 1$$

$$= 0 \qquad \text{for } m = 0 \tag{2-14}$$

and for all m,

$$I_1 = D_{mn} \int_0^{u_{mn}} \left(\frac{mJ_m(x)}{x} \right)^2 x \, dx \qquad (2\text{-}15)$$

where

$$x = k_{cmn} r \qquad (2\text{-}16)$$

$$D_{mn} = \frac{\pi a_{mn}^2 Z_{omn} C_{mn}^2}{k_{cmn}^4} \qquad (2\text{-}17)$$

In a similar manner we obtain

$$I_2 = Z_{omn} \iint h_{rmn}^2 dS = \frac{2D_{mn}}{\epsilon_m} \int_0^{u_{mn}} \left(J'_m(x) \right)^2 x \, dx \qquad (2\text{-}18)$$

where ϵ_m is defined as

$$\epsilon_m = 1 \quad \text{for } m = 0$$
$$\epsilon_m = 2 \quad \text{for } m \geq 1 \qquad (2\text{-}19)$$

The total integral I is

$$I = D_{mn} \int_0^{u_{mn}} \left[\left(\frac{mJ_m(x)}{x} \right)^2 + \frac{2}{\epsilon_m} \left(J'_m(x) \right)^2 \right] x \, dx = 1 \qquad (2\text{-}20)$$

In evaluating Eq. 2-20, the following Bessel function identities will be used:[12]

$$J_o'(x) = -J_1(x) \tag{2-21}$$

$$\frac{2m}{x} J_m(x) = J_{m-1}(x) + J_{m+1}(x) \tag{2-22}$$

$$2J_m'(x) = J_{m-1}(x) - J_{m+1}(x) \tag{2-23}$$

$$\int x J_m^2(x)\, dx = \frac{x^2}{2}\left[J_m^2(x) - J_{m-1}(x) J_{m+1}(x)\right] \tag{2-24}$$

First let m = 0 in Eq. 2-20. Then, with Eqs. 2-19, 2-21, and 2-24

$$I = 2D_{on} \int_0^{u_{mn}} x J_1^2(x)\, dx = D_{on} u_{on}^2 \left[J_1^2(u_{on}) - J_o(u_{on}) J_2(u_{on})\right] \tag{2-25}$$

But u_{on} is defined such that $J_o'(u_{on}) = 0$, or $J_1(u_{on}) = 0$. Therefore,

$$I = - D_{on} u_{on}^2 J_o(u_{on}) J_2(u_{on}) \tag{2-26}$$

Now, by Eq. 2-22

$$J_2(u_{on}) = \frac{2}{u_{on}} J_1(u_{on}) - J_o(u_{on}) = - J_o(u_{on}) \tag{2-27}$$

where use was made of $J_1(u_{on}) = 0$. Hence, for m = 0, the integral I reduces to

$$I = D_{on} u_{on}^2 J_o^2(u_{on}) = 1 \tag{2-28}$$

and with the aid of Eq. 2-17, the coefficient C_{on} is found to be

$$C_{cn} = \frac{k_{con}^2}{\alpha_{on} u_{on} J_o(u_{on})} \sqrt{\frac{1}{\pi Z_{o_{on}}}} \tag{2-29}$$

Now substitute Eqs. 2-6 and 2-10 to obtain

$$C_{on} = \frac{u_{on}}{\pi a^2 J_o(u_{on})} \sqrt{\frac{\lambda}{j2\eta\alpha_{on}}} \tag{2-30}$$

Next let $m \geq 1$ in Eq. 2-20. With Eqs. 2-19, 2-22, and 2-23 substituted in Eq. 2-20, we obtain

$$I = \frac{D_{mn}}{2} \left[\int_0^{u_{mn}} x J_{m-1}^2(x)\, dx + \int_0^{u_{mn}} x J_{m+1}^2(x)\, dx \right], \quad m \geq 1 \tag{2-31}$$

This may be integrated by means of Eq. 2-24 as follows.

$$I = \frac{D_{mn} u_{mn}^2}{4} \Big[J_{m-1}^2(u_{mn}) + J_{m+1}^2(u_{mn}) - J_m(u_{mn}) \left(J_{m-2}(u_{mn}) + J_{m+2}(u_{mn}) \right) \Big], \quad m \geq 1 \tag{2-32}$$

The relations given in Eqs. 2-11, 2-22, and 2-23 allow this to be simplified as given below.

$$I = \frac{D_{mn} u_{mn}^2}{2} J_m^2(u_{mn}) \left(1 - \frac{m^2}{u_{mn}^2}\right) = 1, \quad m \geq 1 \qquad (2\text{-}33)$$

Equation 2-33, with Eqs. 2-6, 2-10, and 2-17, yields

$$C_{mn} = \frac{u_{mn}^2}{\pi a^2 J_m(u_{mn})} \sqrt{\frac{\lambda}{j\alpha_{mn}\eta}} \cdot \frac{1}{\sqrt{u_{mn}^2 - m^2}}, \quad m \geq 1 \qquad (2\text{-}34)$$

Finally, Eqs. 2-30 for C_{on} and 2-34 for C_{mn}, $m \geq 1$, can be combined with the aid of Eq. 2-19. Thus, in general,

$$C_{mn} = \frac{u_{mn}^2}{\pi a^2 J_m(u_{mn})} \sqrt{\frac{\epsilon_m \lambda}{j2\alpha_{mn}\eta}} \cdot \frac{1}{\sqrt{u_{mn}^2 - m^2}}, \quad m \geq 0 \qquad (2\text{-}35)$$

where $\epsilon_m = 1$ for $m = 0$ and $\epsilon_m = 2$ for $m \geq 1$. The normalized magnetic field components for all TE_{mn} modes in circular waveguide are obtained as follows when Eq. 2-35 is substituted in Eqs. 2-7 through 2-9:

$$h_{zmn} = \frac{1}{\pi a^2} \sqrt{\frac{\lambda \epsilon_m}{j2\eta\alpha_{mn}}} \cdot \frac{u_{mn}^2 \cos m\phi}{\sqrt{u_{mn}^2 - m^2}} \cdot \frac{J_m(u_{mn} r/a)}{J_m(u_{mn})} \qquad (2\text{-}36)$$

$$h_{rmn} = -\frac{1}{\pi a} \sqrt{\frac{\alpha_{mn} \lambda \epsilon_m}{j2\eta}} \cdot \frac{u_{mn} \cos m\phi}{\sqrt{u_{mn}^2 - m^2}} \cdot \frac{J'_m(u_{mn} r/a)}{J_m(u_{mn})} \qquad (2\text{-}37)$$

$$h_{\phi mn} = \frac{1}{\pi r} \sqrt{\frac{\alpha_{mn} \lambda \epsilon_m}{j2\eta}} \cdot \frac{m \sin m\phi}{\sqrt{u_{mn}^2 - m^2}} \cdot \frac{J_m(u_{mn} r/a)}{J_m(u_{mn})} \qquad (2\text{-}38)$$

d. Coupling Between Magnetic Dipole Elements

The coefficient a_{mn} in Eq. 2-3 will now be evaluated. By means of Eq. (3-42) of the Second Quarterly Report,[2] a_{mn} is related as follows to h_{zmn}, and the axial magnetic dipole moment m_{1z}

$$a_{mn} = \frac{j\omega\mu_o}{2} h_{zmn} m_{1z} \tag{2-39}$$

The total axial magnetic field at the location of the second dipole due to the dipole moment m_{1z} is given by Eqs. 2-3 and 2-39:

$$H_{2z} = \sum_{mn} \frac{j\omega\mu_o m_{1z}}{2} h_{zmn}^2 e^{-\alpha_{mn} s} \tag{2-40}$$

The coupling coefficient is obtained from Eqs. 2-1 and 2-40.

$$k = -\frac{j\omega\mu_o F}{2} \sum_{mn} h_{zmn}^2 e^{-\alpha_{mn} s} \tag{2-41}$$

On the axis of the circular waveguide, all h_{zmn} components other than h_{zon} are zero. Therefore, Eqs. 2-36 and 2-41 yield

$$k = \frac{F}{2\pi a^4} \sum_{n \geq 1} \frac{u_{on}^2}{\alpha_{on}} \cdot \frac{e^{-\alpha_{on} s}}{J_o^2(u_{on})} \tag{2-42}$$

In going from Eqs. 2-41 to 2-42, $J_o(0) = 1$ and $\omega\lambda\mu_o = 2\pi\eta$ were used. Also, the minus sign was dropped, since -k and k have the same significance in filter design.

e. Coupling Between Dielectric Disks

Equation 2-42 gives the coupling coefficient between a pair of magnetic-dipole elements. In the case of a dielectric disk, the equivalent magnetic-dipole moment is distributed over the volume of the disk. This effect will be taken into account by introducing a distribution factor K_n into each term of the summation in Eq. 2-42. The approach is the same as in the case of axial disks in a rectangular tube, which was analyzed in the Fourth Quarterly Report.[4] Thus

$$k = \frac{F}{2\pi a^4} \sum_{n \geq 1} \frac{K_n u_{on}^2 e^{-\alpha_{on} s}}{\alpha_{on} J_o^2(u_{on})} \tag{2-43}$$

where the distribution factor K_n is given by

$$K_n = \frac{\left(\iint m'_{1z} h_{zon} \, da\right)^2}{\left(\iint m'_{1z} \, da\right)^2} = \frac{1}{m_{1z}^2} \left(\iint m'_{1z} h_{zon} \, da\right)^2 \tag{2-44}$$

Integration in Eq. 2-44 is over the central plane of the disk.

As in the Fourth Quarterly Report, let

$$m'_{1z} \propto J_o\left(\frac{2p_{o1}r}{D}\right) = J_o\left(\frac{4.810r}{D}\right) \tag{2-45}$$

where D is the disk diameter, r is the radial coordinate, and $p_{o1} = 2.405$ is the first root of $J_o(u) = 0$. Now

$$\sqrt{K_n} = A \int_0^{2\pi} \int_0^{D/2} J_o\left(\frac{2p_{o1}r}{D}\right) J_o\left(\frac{u_{on}r}{a}\right) r\, dr\, d\theta$$

$$= 2\pi A \int_0^{D/2} r\, J_o\left(\frac{2p_{o1}r}{D}\right) J_o\left(\frac{u_{on}r}{a}\right) dr \qquad (2\text{-}46)$$

where A is a constant to be evaluated. This can be integrated by means of the following formula[12]

$$\int u\, J_n(\alpha u)\, J_n(\beta u)\, du = \frac{\beta u\, J_n(\alpha u)\, J_{n-1}(\beta u) - \alpha u\, J_{n-1}(\alpha u)\, J_n(\beta u)}{\alpha^2 - \beta^2} \qquad (2\text{-}47)$$

The result is

$$\sqrt{K_n} = 2\pi A \left[\frac{p_{o1}\, J_1(p_{o1})\, J_o\left(\frac{u_{on}D}{2a}\right)}{\left(\frac{2p_{o1}}{D}\right)^2 - \left(\frac{u_{on}}{a}\right)^2} \right] \qquad (2\text{-}48)$$

where use was made of $J_o(p_{o1}) = 0$ and $J_{-1}(u) = -J_1(u)$. Now A may be determined from the fact that K_n must approach one as D/a approaches zero. With A evaluated in this manner, K is given by

$$\sqrt{K_n} = \left[\frac{J_o\left(\frac{u_{on}D}{2a}\right)}{1 - \left(\frac{u_{on}D}{2p_{o1}a}\right)^2} \right]^2 \qquad (2\text{-}49)$$

Therefore, the final formula for the coupling coefficient between an axially oriented pair of dielectric disk resonators in a cut-off circular

tube is as follows:

$$k = \frac{F}{2\pi a^4} \sum_{n \geq 1} \frac{u_{on}^2}{\left[1 - \left(\frac{u_{on} D}{2 p_{o1} a}\right)^2\right]^2} \cdot \frac{J_o^2\left(\frac{u_{on} D}{2a}\right)}{J_o(u_{on})} \cdot \frac{e^{-\sigma_{on} s}}{\alpha_{on}} \qquad (2\text{-}50)$$

where F is given by Eq. 2-2, u_{on} is determined from Eq. 2-11, and $p_{o1} = 2.405$. For convenience in using Eq. 2-50, the first ten values of u_{on} and $J_o(u_{on})$ are tabulated below. (See Ref. 12, p. 166.)

n	u_{on}	$J_o(u_{on})$	n	u_{on}	$J_o(u_{on})$
1	3.832	-0.4028	6	19.616	0.1801
2	7.016	0.3001	7	22.760	-0.1672
3	10.174	-0.2497	8	25.904	0.1567
4	13.324	0.2184	9	29.047	-0.1480
5	16.471	-0.1965	10	32.190	0.1406

f. Comparison Between Theoretical and Experimental Data

Because several approximations were involved in the derivation of Eq. 2-50, its accuracy can only be determined by a comparison of computed coupling-coefficient values with experimental data. For these measurements, a metal tube of inside diameter 0.745" was selected. The same pair of disks was used as in the earlier coupling-coefficient measurements for axial orientation in square tubes.[4] The parameters of the disks are D = 0.393", L = 0.160", ε_r = 97.6, and f_o = 3455 Mc (measured in the 0.745" diameter tube).

Comparison between theoretical and measured coupling-coefficient data for the above case is shown in Figure 2-2 for a wide

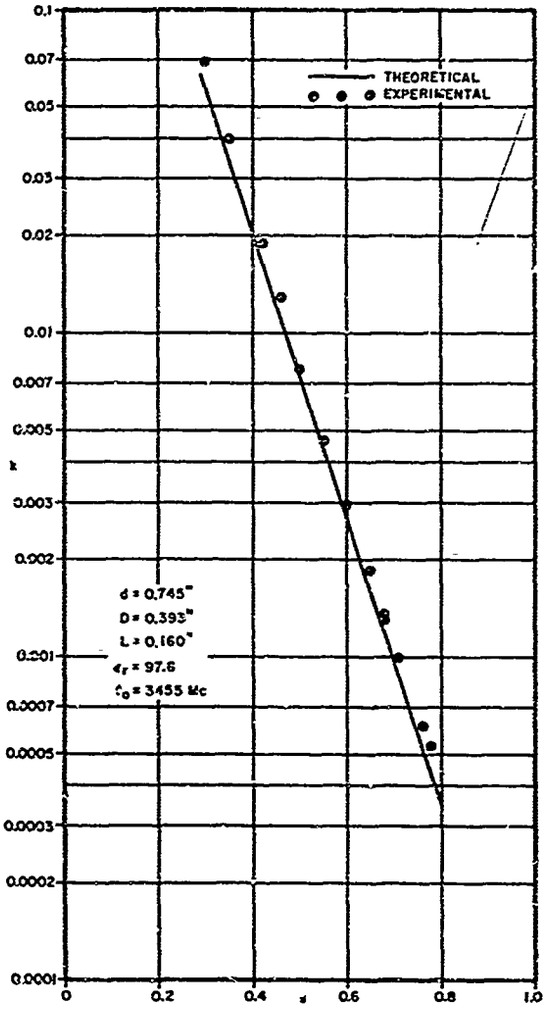

Figure 2-2. Coupling Coefficient versus Center-to-Center Spacing for a Pair of Dielectric-Disk Resonators Axially Oriented in a Circular Cut-Off Tube

range of center-to-center spacings, s. The theoretical curve was computed from Eq. 2-50 with the aid of Eq. 2-2. Convergence of the series in Eq. 2-50 was found to be extremely rapid. Only two terms were required for $s \geq 0.16$", and only one term for $s > 0.6$".

Examination of Figure 2-2 shows that the measured points all lie above the theoretical curve, the average discrepancy being about 14%. Because the slope of the curve is steep, a horizontal displacement of the curve by the small distance $\Delta s = 0.010$" will bring the theoretical and experimental data into close agreement. For most practical purposes the accuracy of Eq. 2-50 is adequate. Where greater accuracy is desired, minor experimental adjustment of the spacings will quickly yield the required filter bandwidth.

3. Band-Stop Resonator in Strip-Line Cross Section

a. General Case in TEM Line

The Fifth Quarterly Report contains a general analysis of a dielectric resonator placed in the field of a propagating TEM

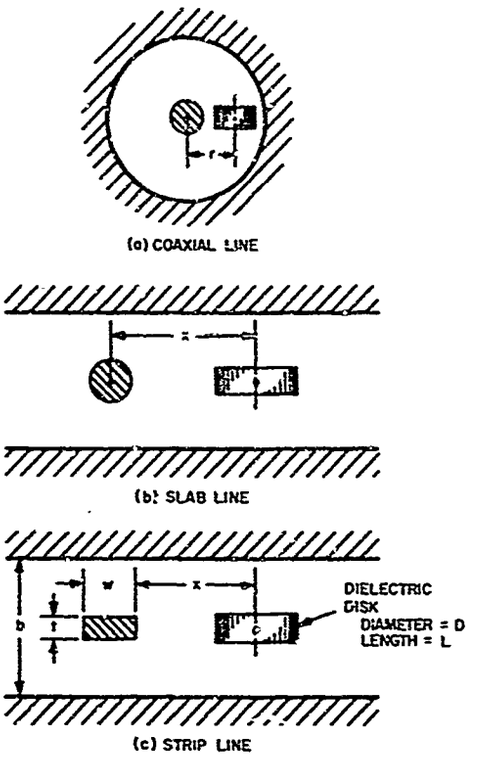

Figure 3-1. Dielectric Resonator Coupled to Various TEM-Mode Lines

transmission line.[5] The effect of this proximity is to introduce a rejection response equivalent to that of a parallel LC circuit in series with the transmission line. Formulas were derived in the Fifth Quarterly Report for the external Q, Q_{ex}, of a dielectric resonator in coaxial-line and slab-line cross sections (Figure 3-1a and b). A formula will now be derived for the strip-line case (Figure 3-1c).

The following general formula holds for Q_{ex} of a dielectric resonator placed in the cross section of any TEM line.

$$Q_{ex} = \frac{\lambda_o Z_o I^2}{\pi F \eta H^2} \qquad (3\text{-}1)$$

where λ_o is the wavelength at resonance, Z_o is the characteristic impedance of the TEM line, I is the electric current carried by the TEM line, F is a constant related to the parameters of the dielectric disk as given by Eq. 2-2, η = 376.6 ohms per square, and H is the magnetic-field value in the TEM-line cross section at the center of the disk. This formula assumes the disk axis to be aligned in the direction of H. If the disk axis is at an angle θ with respect to the vector H, a factor $\cos^2\theta$ should be inserted in the denominator of the formula.

To apply Eq. 3-1 to any particular TEM cross section, it is necessary to evaluate the ratio H/I as a function of the cross-section coordinates. This was done for the coaxial and slab-line cases in the Fifth Quarterly Report, and is done below for the strip-line case.

b. Evaluation of H/I in Strip Line

The ratio H/I in the strip-line cross section will be determined by means of the conformal transformation method.[13] In order to simplify the analysis, we shall assume that the strip is sufficiently wide that the fringing field at one edge is not affected by the proximity of the opposite edge. Previous study of strip line has shown that this assumption holds with good accuracy if $w \geq 0.35(b-t)$. For $\epsilon_r = 1$, this condition requires Z_o to be less than 121 ohms for $t/b = 0$, or less than 86 ohms for $t/b = 0.25$. Since Z_o would usually be about 50 ohms in a band-stop filter, the simplifying assumption will seldom limit the practical utility of the analysis.

As a result of the above assumption, the field distribution in the space adjacent to one edge of the strip will be the same as that of the semi-infinite-plate geometry shown in Figure 3-2a. Because of symmetry, the dashed line is an E-field line and perpendicular to H. Therefore, a magnetic-wall may be inserted along the dashed line, permitting the cross section to be bisected as shown in Figure 3-2b.

The z-plane boundary in Figure 3-2b is transformed into the w-plane boundary in Figure 3-2c by means of[14,15]

$$z = \frac{c}{\pi}\left[\cosh^{-1}\left(\frac{2s-(a+1)}{a-1}\right) - \frac{1}{\sqrt{a}}\cosh^{-1}\left(\frac{(a+1)s-2a}{(a-1)s}\right)\right] - j(c-g) \qquad (3\text{-}2)$$

where

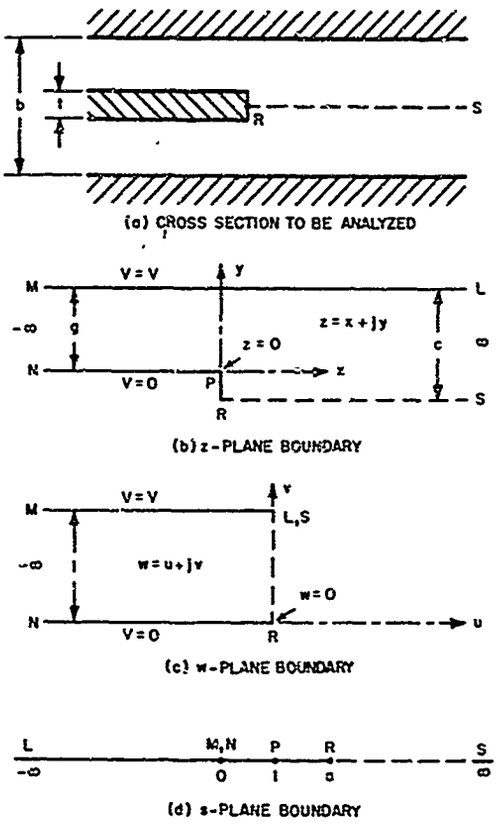

Figure 3-2. Semi-Infinite Plate Geometry and its z, w, and s Plane Equivalents

$$s = a \operatorname{sech}^2\left(\frac{\pi w}{2}\right) \qquad (3\text{-}3)$$

The coordinate systems and important dimensions in the z, w and s planes are defined in Figures 3-2b, c and d. Corresponding points in the three planes are indicated by letters L, M, N, P, R, and S.

The field distribution in the w-plane consists of straight, vertical E lines between the electric-wall boundaries ML and NR, while the H lines are straight and horizontal. Fringing of the field in the region near R and S is prevented by the constraint of the vertical magnetic-wall boundary between those points. Because the electric field is uniform within the w-plane boundary, the field functions in the z-plane are given by the following general formula obtained from basic conformal mapping theory.[13]

$$E = \eta H = K\left|\frac{dw}{dz}\right| \qquad (3\text{-}4)$$

The constant K may easily be evaluated in this case by considering the uniform-field region far to the left of x = 0, where inspection of Figure 3-2 shows that E approaches V/g and dw/dz approaches 1/g. Therefore, K = V and

$$E = \eta H = V \left|\frac{dw}{dz}\right| = V \left|\frac{dw}{ds}\right| \cdot \left|\frac{ds}{dz}\right| \tag{3-5}$$

Differentiation of Eqs. 3-2 and 3-3 yields

$$\frac{dz}{ds} = \frac{c}{\pi} \left\{ \frac{\frac{2}{a-1}}{\left[\left(\frac{2s-(a+1)}{a-1}\right)^2 - 1\right]^{1/2}} - \frac{\frac{2\sqrt{a}}{a-1}}{s\left[\left(\frac{(a+1)\,s-2a}{a-1}\right)^2 - s^2\right]^{1/2}} \right\} \tag{3-6}$$

$$\frac{ds}{dw} = -\pi a \operatorname{sech}^2 \frac{\pi w}{2} \tanh \frac{\pi w}{2} = -\pi s \sqrt{1 - \frac{s}{a}} \tag{3-7}$$

When Eqs. 3-6 and 3-7 are substituted in Eq. 3-5, a formula for H versus the complex variable s is obtained. Equation 3-2 gives the relation between the strip-line cross-section coordinates $z = x + jy$ and s.

The dielectric resonator will now be assumed to be centered symmetrically between the ground planes as shown in Figure 3-1c. Therefore, the field components E and H need only be evaluated along the dashed line RS in Figure 3-2. In this case, the coordinate ranges are $x \geq 0$, $y = -(c - g)$, $u = 0$, $0 \leq v \leq 1$, and $a \leq s \leq \infty$.

Equations 3-2 and 3-5 now become

$$x = \frac{c}{\pi} \left[\cosh^{-1}\left(\frac{2s-(a+1)}{a-1}\right) - \frac{1}{\sqrt{a}} \cosh^{-1}\left(\frac{(a+1)\,s-2a}{(a-1)\,s}\right) \right] \tag{3-8}$$

$$\frac{H}{I} = \frac{Z_o}{\eta} \left|\frac{dv}{ds}\right| \cdot \left|\frac{ds}{dx}\right| \tag{3-9}$$

where use was made of $V = Z_o I$. Equations 3-6, 3-7 and 3-9 combine as follows to yield I/H as a function of s.

$$\frac{I}{H} = \frac{b\eta}{Z_o}\sqrt{\frac{s}{a}-1}\left\{\frac{s}{\left[\left(2s-(a+1)\right)^2-(a-1)^2\right]^{1/2}} - \frac{\sqrt{a}}{\left[\left((a+1)\,s-2a\right)^2-(a-1)^2\,s^2\right]^{1/2}}\right\} \tag{3-10}$$

The position x along the line RS corresponding to s is computed from Eq. 3-8.

c. Computation of Q_{ex} versus x, $0 < x < \infty$

Equations 3-1, 3-8, and 3-10 permit computation of Q_{ex} versus x for any value of x greater than zero. Note that $a = 1/(1-t/b)^2$ and $c = b/2$, where t and b are strip thickness and ground-plane spacing. These expressions can be simplified in the case of x large. By analogy to the slab-line solution,[5] we may anticipate a functional dependence $Q_{ex} \propto e^{2\pi x/b}$ when x exceeds b/2. The simplification for $x > b/2$ is performed below.

d. Computation of Q_{ex} Versus x, $b/2 < x < \infty$

Let x/b and s/a approach infinity in the above equations. Then Eq. 3-10 approaches the limit:

$$\frac{I}{H} = \frac{b\eta}{Z_o}\sqrt{\frac{s}{a}}\left(\frac{1}{2}-\frac{1}{2s}\right)$$

$$= \frac{b\eta}{2Z_c}\sqrt{\frac{s}{a}}, \text{ for } s \longrightarrow \infty \tag{3-11}$$

Simplification of Eq. 3-8 requires the use of the identity

$$\cosh^{-1} A = \log_e \left(A + \sqrt{A^2 - 1} \right) \tag{3-12}$$

Then in the limit $s/a \longrightarrow \infty$

$$\frac{\pi x}{c} = \log_e \left(\frac{4s}{a-1} \right) - \frac{1}{\sqrt{a}} \log_e \left(\frac{a+1}{a-1} + \sqrt{\left(\frac{a+1}{a-1} \right)^2 - 1} \right)$$

$$= \log_e \left(\frac{4s}{a-1} \right) - \frac{1}{\sqrt{a}} \log_e \left(\frac{a+1+\sqrt{4s}}{a-1} \right)$$

$$= \log_e \left(\frac{4s}{a-1} \right) - \frac{1}{\sqrt{a}} \log_e \left(\frac{\sqrt{a}+1}{\sqrt{a}-1} \right)$$

$$= \log_e \left(\frac{4s/a}{\left(1 - 1/\sqrt{a}\right)^{1-1/\sqrt{a}} \left(1 + 1/\sqrt{a}\right)^{1+1/\sqrt{a}}} \right), \text{ for } s \longrightarrow \infty \tag{3-13}$$

Therefore, with $c = b/2$ and $1/\sqrt{a} = 1 - t/b$,

$$\frac{s}{a} = \frac{1}{4} \left(\frac{t}{b} \right)^{\frac{t}{b}} \left(2 - \frac{t}{b} \right)^{2 - \frac{t}{b}} e^{2\pi x/b}, \quad x \longrightarrow \infty \tag{3-14}$$

Equations 3-1, 3-11, 3-14, and $\eta = 120\pi$ yield

$$Q_{ex} = \frac{7.5 \lambda_o b^2}{F Z_o} \left(\frac{t}{b} \right)^{\frac{t}{b}} \left(2 - \frac{t}{b} \right)^{2 - \frac{t}{b}} e^{\frac{2\pi x}{b}}, \quad \frac{x}{b} \longrightarrow \infty \tag{3-15}$$

where F is given by Eq. 2-2 as a function of the dielectric-disk parameters. The range of validity of Eq. 3-15 begins at approximately $x = b/2$.

4. Further Study of Dielectric-Resonator Directional Filters

a. Measurements on Waveguide Dielectric-Resonator Directional Filters

As discussed in the Seventh Quarterly Report,[7] a directional filter is a reciprocal four-port device combining the properties of a directional coupler, a band-pass filter, and a band-stop filter. Figure 4-1 shows a schematic representation of a directional filter and the response at the various ports. Ideally, Port 4 is isolated from Port 1 and Port 3 is isolated from Port 2; furthermore, each port is reflectionless when the other ports are terminated by their Z_o loads.

A number of waveguide directional-filter structures were described and analyzed in the Seventh Quarterly Report.[7] Data on some of these structures are presented below. Figures 4-2 through 4-4 show the configurations measured.

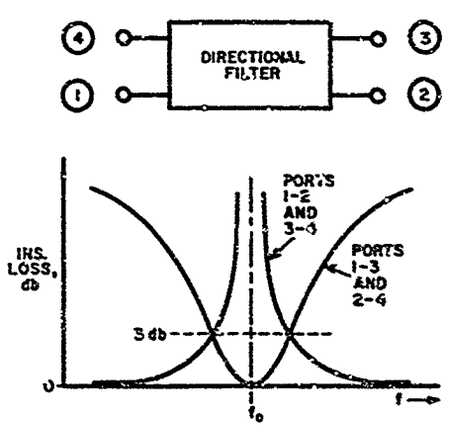

Figure 4-1. Schematic Diagram of Four-Port Directional Filter and Insertion-Loss Response Between Various Pairs of Ports

The response curves for Figure 4-2a appear in Figure 4-5. In this case, two identical disks are used in their first resonant mode. The band-pass and band-stop responses exhibit typical directional-filter behavior. Isolation and VSWR deviate from ideal, but are nevertheless good.

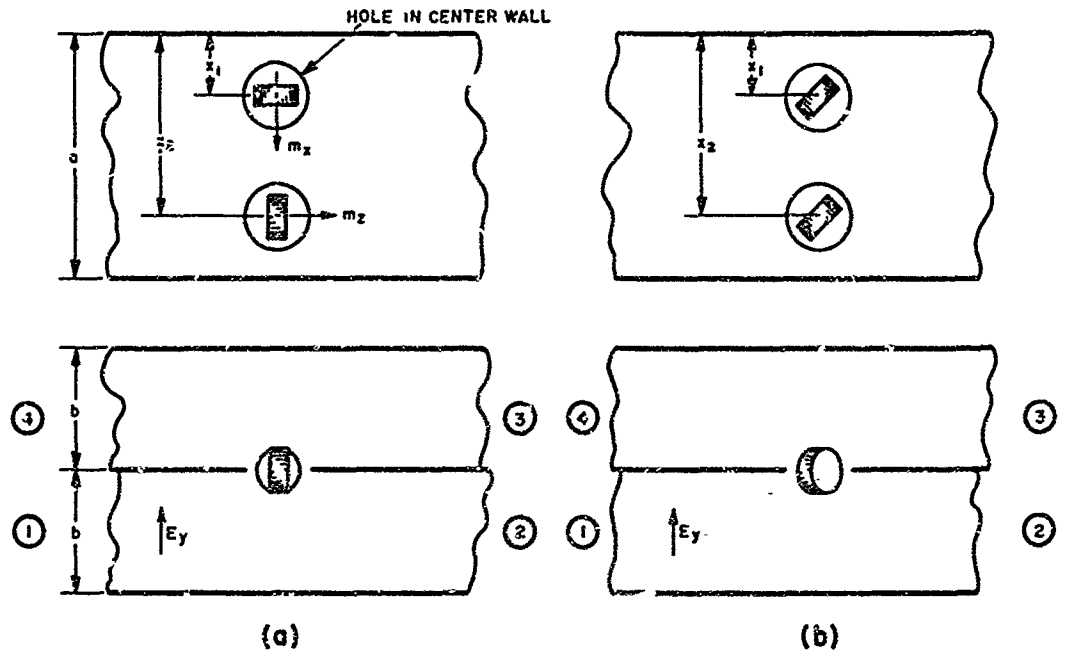

Figure 4-2. Arrangements of Pairs of Dielectric Disks Yielding Directional-Filter Response in Waveguide

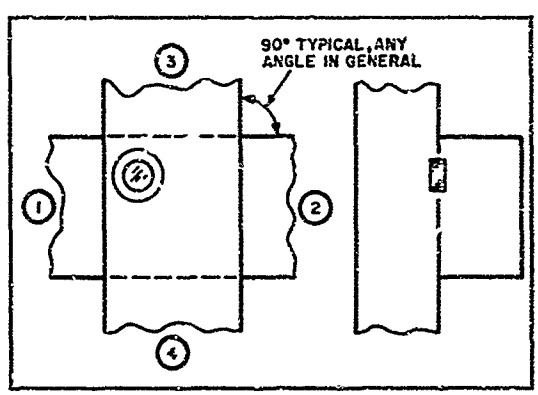

Figure 4-3. Single-Disk, Dual-Mode Configuration Yielding Directional-Filter Response in Waveguide

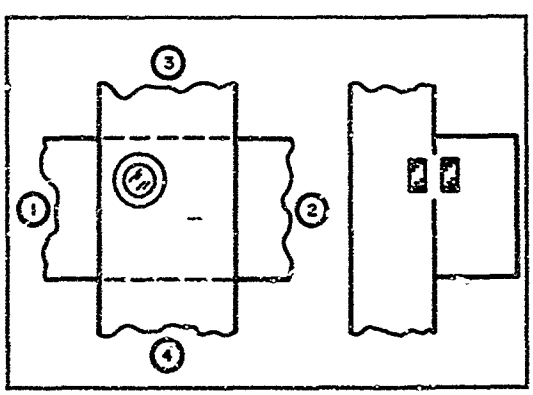

Figure 4-4. Pair of Dual-Mode Disks in a Waveguide Directional Filter

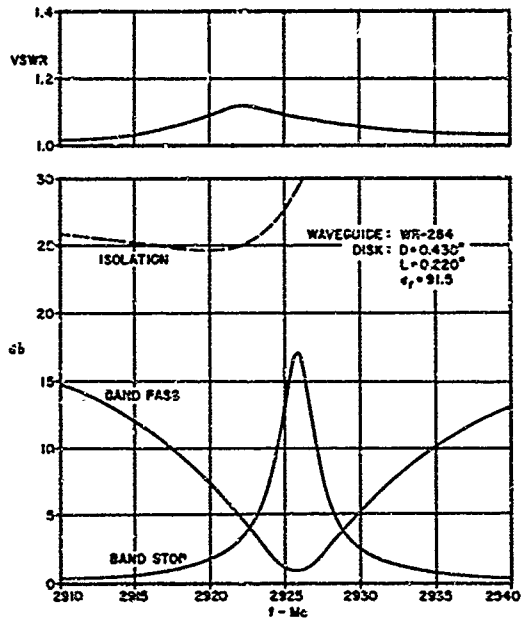

Figure 4-5. Measured Response Curves for Pair of Single-Mode Disks in Directional Filter of Figure 4-2a

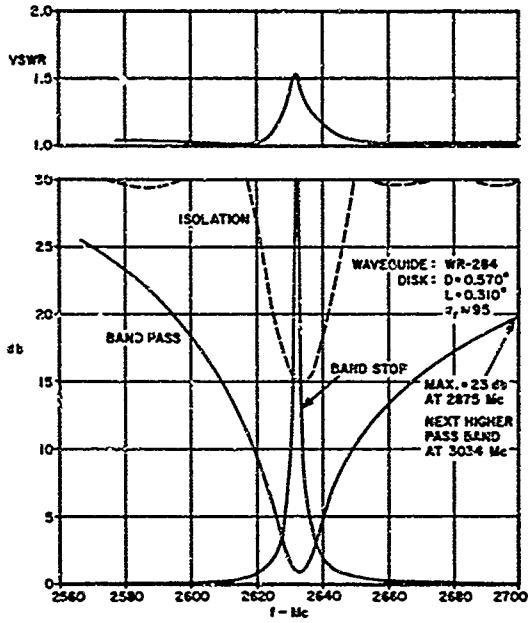

Figure 4-6. Measured Response for One Dual-Mode Disk in Directional Filter of Figure 4-3

The disk arrangement in Figure 4-2b was also tried, but with poor results. Apparently, direct coupling occurring between the two disks was of such magnitude as to seriously affect proper performance. Although band-pass and band-stop responses were observed, the isolation and VSWR were very poor. Because of the success with Figure 4-2a, Figure 4-2b was not pursued further.

Response curves for the single-disk dual-mode case in Figure 4-3 are given in Figure 4-6. Quite satisfactory directional-filter performance was obtained, although the isolation and VSWR are inferior to that of Figures 4-2 and 4-5.

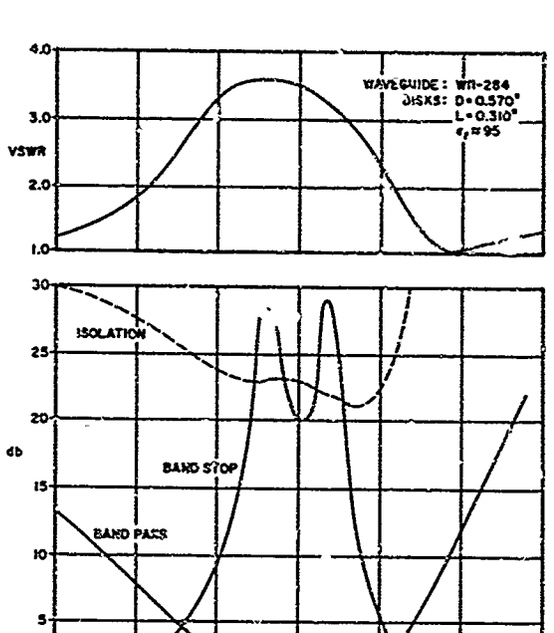

Figure 4-7. Measured Response for Two Dual-Mode Disks in Directional Filter of Figure 4-4

The last case tested is that of the two coupled dual-mode disks of Figure 4-4. As anticipated, the band-pass and band-rejection curves are typical of the response achieved with two-port filters utilizing two resonators. The isolation is quite good, but the VSWR is poor.

The superior results achieved with single-mode disks is not surprising. With a pair of single-mode disks, independent control is achieved over resonant frequency and loaded Q of the two resonant modes. With dual-mode disks, there is a much more complex problem in achieving identical values of resonant frequency and loaded Q of the two modes, and furthermore there is considerably greater difficulty in eliminating direct coupling between the two modes in each disk. When two dual-mode disks are used, the difficulty is increased still further. Thus, the results plotted in Figure 4-7 were obtained after lengthy, tedious adjustment. It was found that a simultaneous condition of good performance on all parameters could not be achieved with a reasonable amount of effort. The curves in Figure 4-7 represent a compromise in which VSWR was sacrificed in favor of the other responses.

b. Strip-Line and Slab-Line Directional Filters

Figure 4-8 shows several strip-line (or slab-line) directional-filter circuits utilizing dielectric resonators. Circuit (a) is

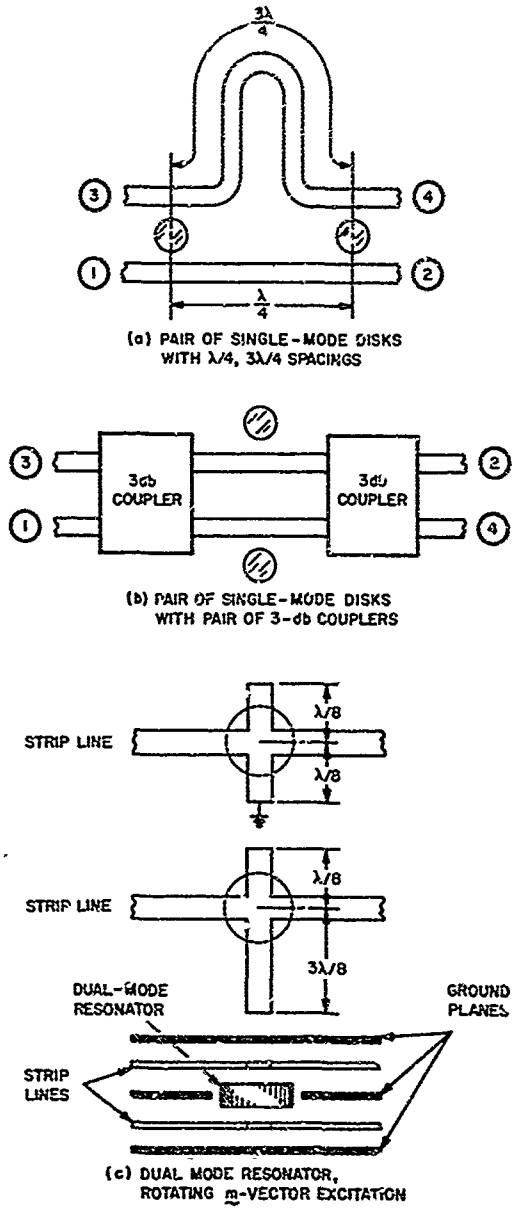

Figure 4-8. Three Strip-Line (or Slab-Line) Circuits Providing Directional-Filter Performance with Dielectric Resonators

analogous to the well-known half-wave-strip directional filter.[16] Circuit (b) uses a pair of cascaded 3-db couplers with rejection resonators coupled to the connecting arms. This is analogous to a type of directional filter widely used in microwave communication systems.[17] Circuit (c) contains a dual-mode resonator coupled to the primary and secondary circuits in a manner that excites a circularly polarized rotating $\underset{\sim}{m}$ vector in the disk. The principle of operation of this case is similar to that of the circularly polarized waveguide-cavity type of directional filter.[16]

The directional-filter circuit in Figure 4-8a will now be analyzed by the method of even and odd excitations.[16] The two excitations on the two strip lines are shown in Figure 4-9. It is clear that the odd excitation couples to the axial $\underset{\sim}{m}$ vector of the disk, while zero coupling occurs for the even excitation. The reflection coefficient r and transmission coefficient t apply at the indicated reference plane.

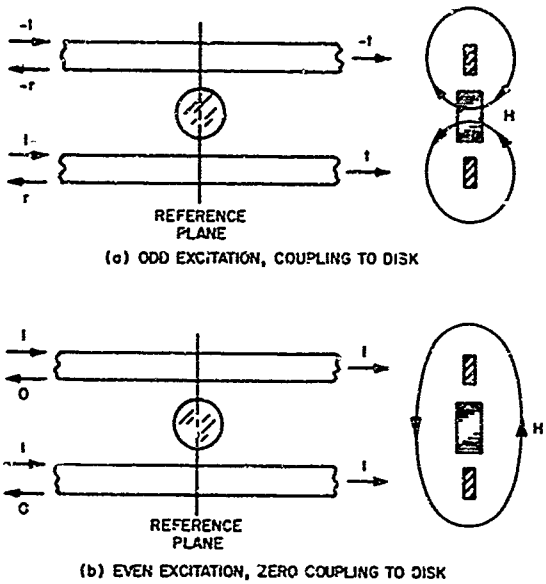

Figure 4-9. Even and Odd Excitations

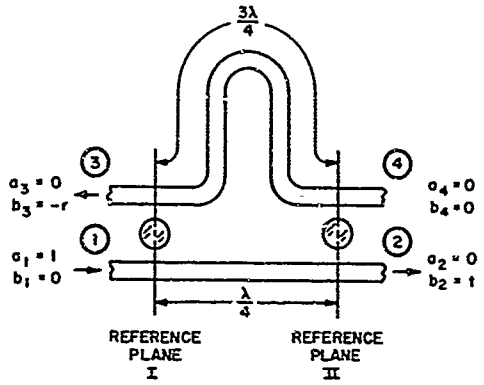

Figure 4-10. Schematic Diagram Showing Wave Amplitudes

In Figure 4-10, in-going wave amplitudes at the four ports are a_1, a_2, a_3, a_4, while out-going wave amplitudes are b_1, b_2, b_3, b_4. Let Port 1 be the input port. Then the desired conditions $a_1 = 1$ and $a_2 = a_3 = a_4 = 0$ are satisfied by superimposing one-half unit each of the odd and even excitations of Figure 4-9. The disk at Reference Plane I in Figure 4-10 couples only to the odd excitation. Note that the excitations at Reference Plane II are reversed due to the $\lambda/2$ difference of length of the two strip lines between Planes I and II. Therefore, the second disk couples only to the even excitation of Ports 1 and 3. The superimposed half-unit excitations at the four ports are as follows with respect to Reference Plane I:

$$a_1 = 1/2 + 1/2 = 1$$

$$b_1 = \frac{r}{2} + \frac{r}{2}\angle -180^\circ = 0$$

$$a_3 = 1/2 - 1/2 = 0$$

$$b_3 = -\frac{r}{2} + \frac{r}{2}\angle -540^\circ = -r$$

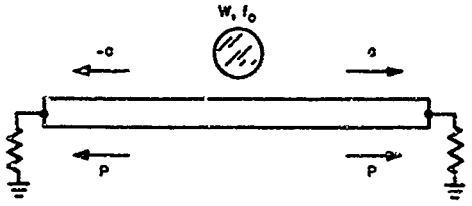

(a) RESONANT DISK COUPLED TO ONE STRIP

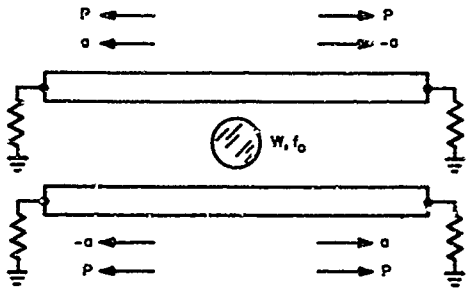

(b) RESONANT DISK COUPLED TO TWO STRIPS

Figure 4-11. Amplitudes and Powers Coupled into Adjacent Strip Lines by Energized Resonant Disks

$$a_2 = 0$$

$$b_2 = \frac{t}{2} + \frac{t}{2} = t$$

$$a_4 = 0$$

$$b_4 = \frac{t}{2} - \frac{t}{2} = 0$$

These wave amplitudes are shown on the circuit in Figure 4-10, and conform to ideal directional-filter behavior. At resonance, r = 1 and t = 0, while far from resonance $r \to 0$ and $t \to 1$. Therefore, the response sketched in Figure 4-1 is obtained.

The bandwidth of the directional-filter response curves will now be related to the bandwidth of a single-reconator band-stop filter. First assume the dielectric disk to be oscillating at its resonant frequency f_o with energy W, as shown in Figure 4-11a. Its external magnetic field will induce waves of amplitude a and -a traveling to the right and left. The total power dissipated is 2P, where P is the power contained in each wave. Since $Q_{ex} = \omega W / P_d$ and $P_d = 2P$,

$$\left(Q_{ex}\right)_{BSF} = \frac{\omega W}{2P}$$

Now consider Figure 4-11b where the disk is coupled to two strip lines as in the directional filter. The spacings, and other dimensions are assumed the same as in the case of the band-stop filter. Therefore,

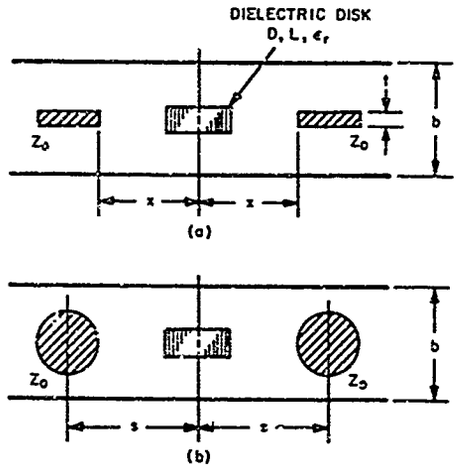

Figure 4-12. Strip- and Slab-Line Cross Sections Used in Dielectric-Resonator Directional Filter

four waves of amplitude a or -a are induced, and the total dissipated power is 4P. The external Q of the disk is

$$\left(Q_{ex}\right)_{DF} = \frac{\omega W}{4P}$$

Hence

$$\left(Q_{ex}\right)_{DF} = \frac{1}{2}\left(Q_{ex}\right)_{BSF} \tag{4-1}$$

and

$$\left(\frac{BW_{3db}}{f_o}\right)_{DF} = 2\left(\frac{BW_{3db}}{f_o}\right)_{BSF} \tag{4-2}$$

Now the formula for Q_{ex} of a band-stop resonator, Eq. 3-15, may be used to yield the 3-db bandwidth of the corresponding directional filter. Thus,

$$\left(\frac{BW_{3db}}{f_o}\right)_{DF} = \frac{F Z_o e^{-2\pi x/b}}{3.75\lambda_o b^2 \left(\frac{t}{b}\right)^{t/b} \left(2-\frac{t}{b}\right)^{2-t/b}} \tag{4-3}$$

where $x \geq b/2$ and $w \geq 0.35(b-t)$. The symbols b, t, and x are defined in Figure 4-12a, while F is given by Eq. 2-2.

For the slab-line case, Eq. (3-4) of the Fifth Quarterly Report may be used to yield

$$\left(\frac{BW_{3db}}{f_o}\right)_{DF} = \frac{60\pi^2 F}{Z_o \lambda_o b^2 \sinh^2\left(\frac{\pi s}{b}\right)} \qquad (4\text{-}4)$$

where $Z_o \geq 50$ ohms. The symbols b and s are defined in Figure 4-12b.

5. Band-Pass Filters in Strip or Slab Line

Figure 5-1 shows how dielectric-resonator band-pass filters may be constructed in strip or slab line. Since magnetic-field coupling is necessary with dielectric resonators, the resonator should be located near a maximum current point on the adjacent strip. This condition can be achieved by ending the strip in a short circuit near the resonator, or in an open circuit a quarter wavelength beyond the resonator.

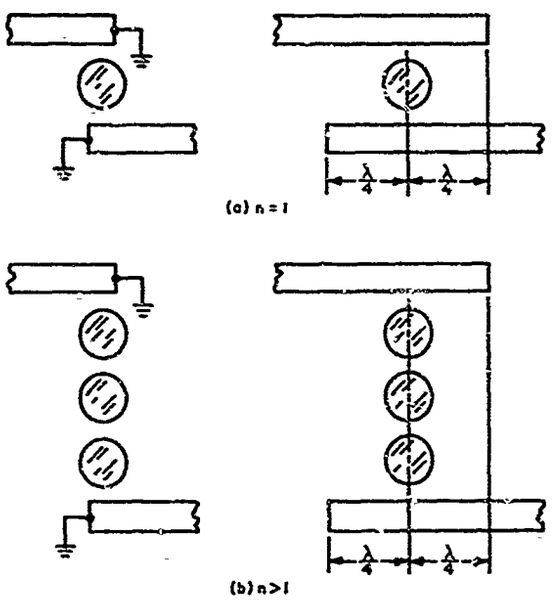

Figure 5-1. Examples of Dielectric-Resonator, Band-Pass Filters with Strip-Line Terminations

The external loading of a resonator is a necessary quantity in the design of a band-pass filter. The parameter used to express this loading is Q_{ex1}, where the subscript "1" denotes loading by one termination, only. There is a close relationship between the cases of band-stop and band-pass resonators coupled to a line. This relationship is apparent from Figure 5-2. The essential difference between the two cases is that the adjacent line is terminated by Z_o at both ends in the band-stop case, and at one end in the band-pass case. From the equivalent circuits in Figure 5-2, it is apparent that

$$\left(Q_{ex1}\right)_{BPF} = \frac{1}{2}\left(Q_{ex}\right)_{BSF} \qquad (5\text{-}1)$$

This equation assumes, of course, that the dielectric resonators are identical, and that all dimensions are the same.

A resonator in the n = 1 band-pass case is loaded by two terminations, so that

$$\frac{f_o}{BW_{3db}} = \left(Q_{ex}\right)_{BPF} = \frac{1}{2}\left(Q_{ex1}\right)_{BPF} = \frac{1}{4}\left(Q_{ex}\right)_{BSF} \qquad (5\text{-}2)$$

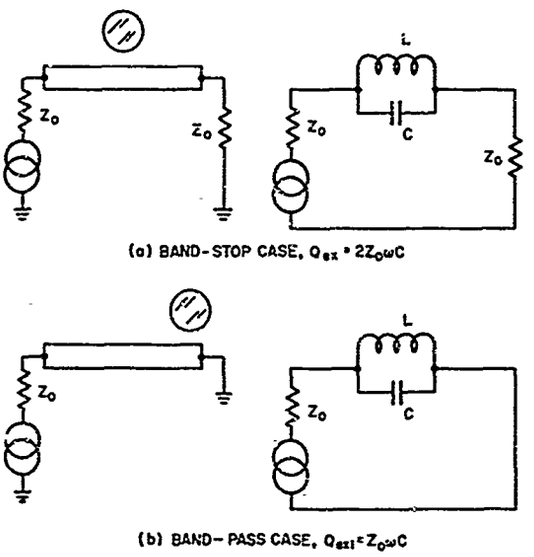

Figure 5-2. Equivalent Circuits, Band-Pass and Band-Stop Cases

The design of a multiple-resonator (n > 1) band-pass filter for a given bandwidth and response function can be accomplished in terms of Q_{ex1} at each end of the filter, and the coupling coefficients k_{12}, k_{23}, etc., between the resonators.[18-20] The parameter Q_{ex1} may be evaluated by means of Eq. 5-1 and either Eq. (3-15) for the strip-line band-stop case or Eq. (3-4) of the Fifth Quarterly Report[5] for the slab-line band-stop case. A formula for the coupling coefficient between two resonators in a region bounded by two ground planes has not yet been derived. Until a suitable formula becomes available, experimental coupling-coefficient data must be used.

6. Diplexers in Strip or Slab Line

A diplexer filter is a three-port component used to separate or combine signals of different frequencies. Diplexers may be formed by joining a pair of two-port filters at a common junction. Figure 6-1 shows several such combinations of two-port band-pass and band-stop filters, and indicates the frequency behavior of each diplexer.

Care must be taken in joining the individual two-port filters to achieve satisfactory VSWR in the desired frequency bands. When the channel spacing is wide compared to the bandwidths, the problem is simple. With moderately close spacing, the presence of one filter will appreciably affect the performance of the other, but minor empirical adjustments will usually yield low VSWR in the pass bands. With very close spacing, it is often necessary to design the circuit specifically as a diplexer, rather than as separate two-port channels.[18] An alternative approach is to use a four-port directional filter as a diplexer, while another approach is to use a three-port circulator connected to a band-pass, band-stop, low-pass, or high-pass filter (Figure 6-2). Each of these approaches automatically provides matched pass bands. Note that the circulator-filter type of diplexer is nonreciprocal, which may in some cases be a disadvantage.

The various cases in Figure 6-1 will be discussed under the assumption that the channel-spacing-to-bandwidth ratios are sufficient to permit simple joining of two-port filters. Figure 6-1a shows two band-pass filters coupled to a common strip line. At the center frequency of each resonator, the other resonator is far from resonance, and therefore the reactance it couples into the strip line is too small to be important. The design method described in Sub-section 5, above, may be used to achieve the desired bandwidth of each channel.

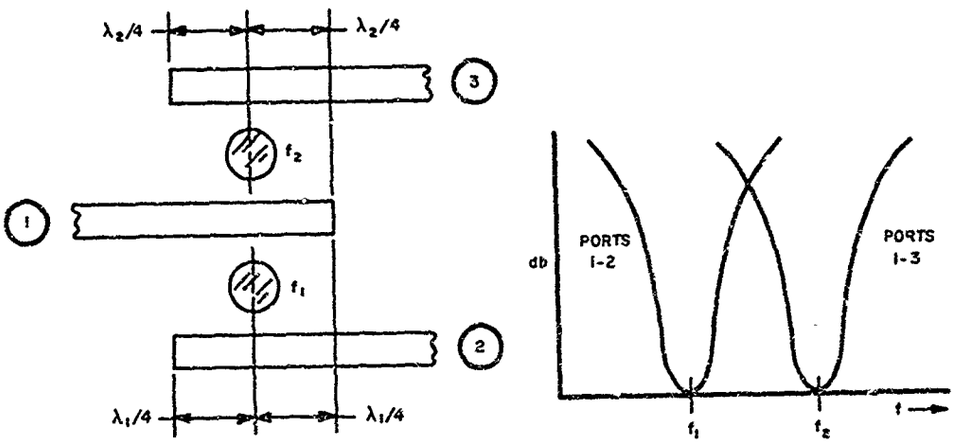

(a) BAND-PASS, BAND-PASS TYPE

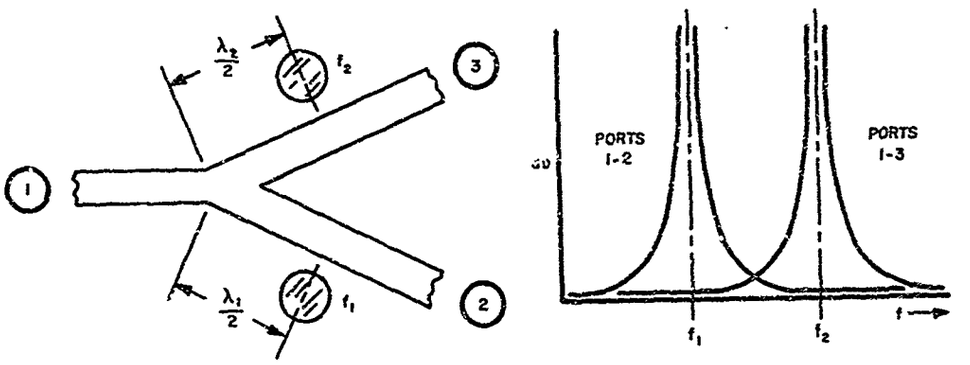

(b) BAND-STOP, BAND-STOP TYPE

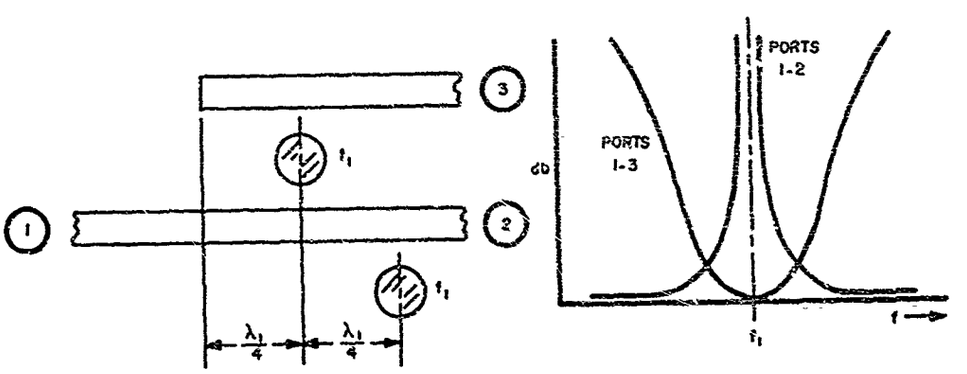

(c) BAND-PASS, BAND-STOP TYPE

Figure 6-1. Examples of Three Basic Diplexer Circuits

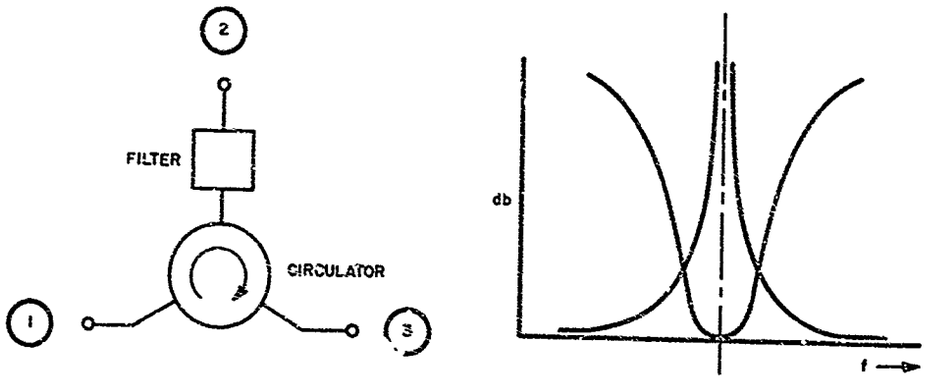

Figure 6-2. Circulator-Filter Type of Diplexer

Figure 6-1b shows a diplexer consisting of two band-stop filters. At f_1, the lower resonator introduces an open circuit in series with the adjacent line. Therefore, at the junction point $\lambda/2$ away, the lower line presents negligible shunt admittance, and a signal at frequency f_1 will pass between Ports 1 and 3 with very little reflection or dissipation loss. At frequency f_2, the situation is reversed. The desired band-stop bandwidths may be achieved by the techniques and formulas contained in the Fifth Quarterly Report[5] and in Sub-section 3, above.

A band-pass and band-stop filter are combined to form a diplexer in Figure 6-1c. Note that both resonators are tuned to f_1. In the case of a signal sufficiently far from f_1, the resonators are virtually unexcited, and Port 1 to Port 2 is a low-loss path. At f_1, the lower resonator introduces an open circuit in series with the lower line, and causes a short-circuit (high-current) point to occur at the location of the upper resonator. Therefore, Port 1 to Port 3 is a band-pass path centered at f_1. The bandwidths of the band-pass and band-stop filters may be related to dimensions by means of the techniques discussed above.

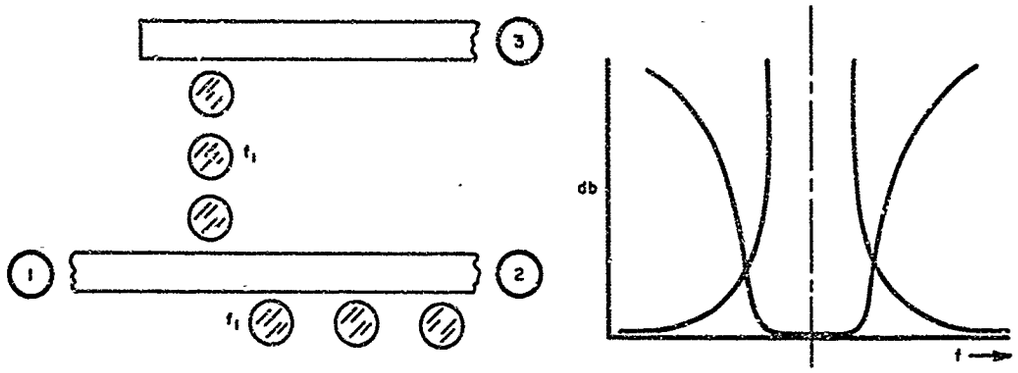

Figure 6-3. Example of Multiple-Resonator Design

The various band-stop and band-pass filters in Figure 6-1 have one resonator; that is, n 1. If desired, the selectivity of the channels may be improved by utilizing multiple-resonator filters (n > 1). An example is shown in Figure 6-3, which combines an n = 3 band-pass filter with an n = 3 band-stop filter. Design approaches for multiple-resonator band-stop and band-pass filters are given in the Fifth Quarterly Report, and in Sub-section 3, above.

7. End Coupling in an Axially Oriented Band-Pass Filter

Formulas for the coupling coefficient between axially oriented dielectric resonators spaced along the center-line of a cut-off rectangular or circular metal tube are derived in Sub-section 2, above, and in Sub-section 2 of the Fourth Quarterly Report.[4] In order to achieve a band-pass filter response with this geometry, end couplings to terminating lines must be provided. The subject of end couplings has already been studied in connection with transverse orientation in a rectangular cut-off tube[4] and with strip- or slab-line geometries (Sub-section 5, above). The axial-orientation case has been found to have special problems, however.

In the transverse-orientation case, end loadings can be achieved that are suitable for bandwidths up to about 2%. In the axial-orientation case, however, the end loadings achieved experimentally are smaller, yielding bandwidths under 1%.

The basic difficulty in achieving large couplings to an axially oriented dielectric resonator is use of a higher-order waveguide mode as the principal coupling mode. In square waveguide this mode is the TE_{20}, while in circular waveguide it is the TE_{01}. These, respectively, have cut-off frequencies and attenuation constants 2.0 and 2.08 times that of the fundamental TE_{10} and TE_{11} modes. Use of the higher mode causes several difficulties in comparison to the use of the fundamental mode in the transverse-orientation case. (1) The larger attenuation constant requires closer spacing of the coupling loop to the resonant disk. For the closest possible spacing, where the loop is in contact with the disk, less coupling will be obtained. (2) The more complex field distribution of the higher mode in the waveguide cross section results in a reduction in the effective area of a large loop, which further reduces maximum coupling in the axial orientation case. (3) Unless a difficult-to-build, elaborate coupling means is used, the fundamental mode will be strongly excited, reducing the coupling for the desired higher mode. Also, because of the relatively low attenuation of the fundamental mode, direct coupling between the end-coupling elements at the two ends of the filter may reduce the attainable stop-band insertion loss below a tolerable value. The latter disadvantage may be minimized, however, by positioning the end-coupling elements with a relative 90° rotation about the waveguide axis so that their TE_{10} excitations will be cross polarized.

Figure 7-1 shows two coupling configurations that were tested experimentally. In both cases, the internal cross section of the square tube was 0.750" by 0.750". The parameters of the resonant disk were

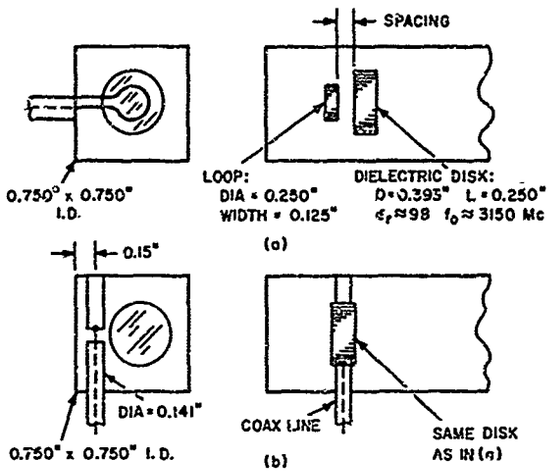

Figure 7-1. End-Coupling Structures Investigated, Axial Orientation of Disk

D = 0.393", L = 0.250", $\epsilon_r \approx 98$, $f_o \approx 3150$ Mc. With the loop shown in Figure 7-1a, the measured external Q, Q_{ex} versus spacing is as given below:

Spacing	Q_{ex}
0.027"	495
0.52	476
0.62	594
0.77	643

The minimum value of Q_{ex} is 476. A band-pass filter designed with this value would have a bandwidth of about 0.2%. Increasing the diameter of the loop decreased the minimum-attainable Q_{ex} to about 200 with the diameter slightly smaller than the diameter of the disk. A larger loop resulted in an increase in Q_{ex}, signifying a decrease of coupling. Minimum Q_{ex} for a loop larger than the disk was obtained with a slight positive spacing, rather than with an overlap condition.

The second coupling element, shown in Figure 7-1b is a center-driven inductive post fed by a coaxial line. This excites the TE_{10} and TE_{20} waveguide modes quite strongly. Minimum Q_{ex} of about 220 was obtained when the post and disk were in the same cross-section plane, as indicated in the figure. This would permit a bandwidth of about 0.5%.

Figure 7-2 shows a symmetrical-post configuration that results in about one half the Q_{ex} value of Figure 7-1b. In addition to the advantage of two coupling elements, the performance benefits from discrimination against TE_{10} excitation. Any device or circuit that drives

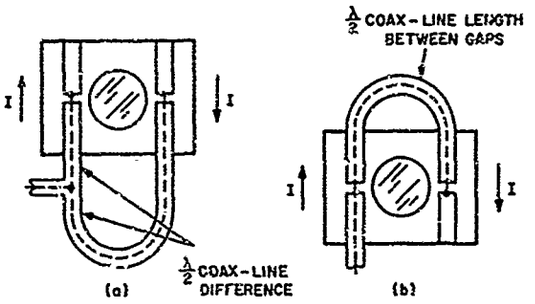

Figure 7-2. Double-Post Excitation of Axial Disk

the posts in equal amplitude and opposite phase may be used. One additional means of achieving this excitation is shown in Figure 7-2b.

At this point one may conclude that transverse orientation of dielectric resonators has practical advantages over axial orientation. With transverse orientation, greater bandwidth is achievable for a given complexity of end-coupling structure; the fundamental waveguide mode is utilized rather than requiring suppression; resonator tuning is more easily accomplished; and positioning of the resonators is less critical.

SECTION V

CONCLUSIONS

This program of investigation of microwave dielectric-resonator filters is now complete. The goal of establishing feasibility and design criteria for high-Q, miniature dielectric resonators in various types of filters has been successfully accomplished. An important problem requiring study and solution before these filters can be used in practical applications is that of temperature sensitivity. Possible approaches to solve this problem are improvement of materials, temperature regulation, and compensation through proximity of other elements offering the opposite change with temperature.

During the final quarter, a theoretical formula was derived for the coupling coefficient between axially oriented dielectric disks in a circular cut-off tube. Agreement with experimental data showed this equation to be adequate for ordinary design purposes. Theoretical analyses were also successful for band-stop disk resonators in strip line, and for band-pass disk resonators coupled to strip and slab line.

Directional-filter performance was verified experimentally for several of the waveguide configurations analyzed in the Seventh Quarterly Report.[7] As expected, adjustment proved easier for single-mode disks than for dual-mode disks. The n = 2, dual-mode configuration was especially difficult, and may be too complex to be practical.

Diplexers offering various types of response are feasible with dielectric resonators. The design of diplexers is simple when the channel separation is at least several times the channel bandwidth. When the channel separation and bandwidth are more nearly equal, more complex structures and adjustments are necessary. This

difficulty may be circumvented by using directional filters or circulator-filter combinations as diplexers.

End coupling in the case of axially oriented disks is subject to difficulties not present in the transverse case. To achieve bandwidths exceeding a few tenths of a percent, complex end structures must be used with axial orientation. The maximum band-pass-filter bandwidth is on the order of one percent compared to about two percent for far simpler structures exciting transverse disks. An additional problem in the axial case is excitation of the fundamental waveguide mode by the end structures. This mode is not utilized in coupling between axially oriented disk resonators, the principal mode being the TE_{20} in rectangular waveguide and TE_{01} in circular waveguide. In the transverse case, the fundamental mode is the principal mode of coupling between resonators as well as to the end structures.

SECTION VI

LIST OF REFERENCES

1. S. B. Cohn and C. W. Chandler, "Investigation of Microwave Dielectric-Resonator Filters", First Quarterly Report on Contract DA-36-039-AMC-02267(E), 1 July 1963 to 30 September 1963, Rantec Corp., Project 31625.

2. S. B. Cohn and K. C. Kelly, "Investigation of Microwave Dielectric-Resonator Filters", Second Quarterly Report on Contract DA-36-039-AMC-02267(E), 1 October 1963 to 31 December 1963, Rantec Corp., Project 31625.

3. S. B. Cohn and K. C. Kelly, "Investigation of Microwave Dielectric-Resonator Filters", Third Quarterly Report on Contract DA-36-039-AMC-02267(E), 1 January 1964 to 31 March 1964, Rantec Corp., Project 31625.

4. S. B. Cohn and E. N. Torgow, "Investigation of Microwave Dielectric-Resonator Filters", Fourth Quarterly Report on Contract DA-36-039-AMC-02267(E), 1 April 1964 to 31 August 1964, Rantec Corp., Project 31625.

5. S. B. Cohn and E. N. Torgow, "Investigation of Microwave Dielectric-Resonator Filters", Fifth Quarterly Report on Contract DA-36-039-AMC-02267(E), 1 September 1964 to 30 November 1964, Rantec Corp., Project 31625.

6. S. B. Cohn and E. N. Torgow, "Investigation of Microwave Dielectric-Resonator Filters", Sixth Quarterly Report on Contract DA-36-039-AMC-02267(E), 1 December 1964 to 28 February 1965, Rantec Corp., Project 31625.

7. S. B. Cohn and E. N. Torgow, "Investigation of Microwave Dielectric-Resonator Filters", Seventh Quarterly Report on Contract DA-36-039-AMC-02267(E), 1 March 1965 to 31 May 1965, Rantec Corp., Project 31625.

8. R. D. Richtmeyer, Journ. of Appl. Phys., Vol. 10, 1939.

9. H. M. Schlicke, "Quasi-Degenerated Modes in High-Dielectric Cavities," Journ. of Appl. Phys., Vol. 24, Feb., 1953.

10. A. Okaya and L. F. Barash, "The Dielectric Microwave Resonator," Columbia Radiation Laboratory Report, Columbia University, New York, N.Y. Also Proc. IRE, Vol. 50, Oct. 1962.

11. S. Ramo and J. R. Whinnery, "Fields and Waves in Modern Radio," 2nd Ed.; John Wiley and Sons, Inc., New York, 1953.

12. E. Jahnke and F. Emde, "Tables of Functions," Dover Publications, New York, 1943; pp. 144-146.

13. E. Weber, "Electromagnetic Fields, Theory and Applications," Vol. I — Mapping of Fields, John Wiley and Sons, Inc., New York, 1950.

14. S. B. Cohn, unpublished notes, Nov. 23, 1953. The derivation of Eqs. 3-2 and 3-3 is carried out in these notes as an extension of the solution for a related geometry treated in Ref. 15 by M. Walker.

15. M. Walker, "Conjugate Functions for Engineers," Oxford University Press, 1933.

16. S. B. Cohn and F. S. Coale, "Directional Channel-Separation Filters," Proc. IRE, Vol. 44, pp. 1018-1024; Aug., 1956.

17. W. D. Lewis and L. C. Tillotson, "A Non-Reflecting Branching Filter for Microwaves," BSTJ, Vol. 27, pp. 83-96; January, 1948.

18. G. L. Matthaei, L. Young, and E. M. T. Jones, "Microwave Filters, Impedance-Matching Networks, and Coupling Structures," McGraw-Hill Book Co., New York, 1964; Chap. 16.

19. "Reference Data for Radio Engineers," 4th Ed., International Telephone and Telegraph Corp., New York, 1956; pp. 218-221.

20. S. B. Cohn, "Direct-Coupled-Resonator Filters," Proc. IRE, Vol. 45, pp. 187-196, February 1957.

SECTION VII

IDENTIFICATION OF KEY TECHNICAL PERSONNEL

	Hours
Dr. Seymour B. Cohn Specialist	164
Mr. Eugene N. Torgow Staff Engineer	71
Mr. Samuel A. Rosen Staff Engineer	40
Mr. Richard V. Reed Engineer	153
Mr. William N. Levin Engineer	44.5
Mr. Howard V. Stein Junior Engineer	32

Security Classification

DOCUMENT CONTROL DATA - R&D

(Security classification of title, body of abstract and indexing annotation must be entered when the overall report is classified)

1. ORIGINATING ACTIVITY (Corporate author)	2a. REPORT SECURITY CLASSIFICATION
Rantec Corporation Calabasas, California	Unclassified
	2b GROUP

3. REPORT TITLE

Investigation of Microwave Dielectric-Resonator Filters

4. DESCRIPTIVE NOTES (Type of report and inclusive dates)

Final Report 1 June 1965 - 31 December 1965

5. AUTHOR(S) (Last name, first name, initial)

Cohn, Seymour B.

6. REPORT DATE	7a TOTAL NO. OF PAGES	7b. NO. OF REFS
May 1966	50	20

8a. CONTRACT OR GRANT NO.	9a. ORIGINATOR'S REPORT NUMBER(S)
DA 36-039-AMC-02267(E) b. PROJECT NO. 1P6 22001 A 057 c. 1P6 22001 A 057 02 d.	9b. OTHER REPORT NO(S) (Any other numbers that may be assigned this report) ECOM-02267-F

10. AVAILABILITY/LIMITATION NOTICES

Each transmittal of this document outside the Department of Defense must have prior approval of CG, U. S. Army Electronics Command, Fort Monmouth, N. J., AMSEL-KL-EM

11. SUPPLEMENTARY NOTES	12. SPONSORING MILITARY ACTIVITY
	U. S. Army Electronics Command Fort Monmouth, New Jersey AMSEL-KL-EM

13. ABSTRACT

Coupling between dielectric-disk resonators, which are axially oriented along the center line of a cut-off circular tube, has been analyzed and a coupling coefficient formula has been derived. The accuracy of the formula is sufficient for most practical purposes.

A band-stop dielectric-disk resonator coupled to a propagating strip line is treated and the formula for external Q, Q_{ex}, is derived.

Response curves are given for three waveguide directional filters utilizing dielectric resonators, which in all cases verified directional filter behavior. The configurations tried were: a pair of single-mode disks, one dual-mode disk, and two dual-mode disks. Several TEM-line directional filters also are discussed.

External loading of the end resonators of a multiple disk band pass filter is studied in the case of a parallel plane boundary and formulas for Q_{ex} are derived.

Various techniques are described for joining band-pass and band-stop filters to form three-port diplexers.

DD FORM 1 JAN 64 1473

Security Classification

Security Classification

14. KEY WORDS	LINK A		LINK B		LINK C	
	ROLE	WT	ROLE	WT	ROLE	WT
Filter						
Dielectric						
Resonator						
Dielectric Resonator						
Directional Filter						
Diplexer						

INSTRUCTIONS

1. ORIGINATING ACTIVITY: Enter the name and address of the contractor, subcontractor, grantee, Department of Defense activity or other organization *(corporate author)* issuing the report.

2a. REPORT SECURITY CLASSIFICATION: Enter the overall security classification of the report. Indicate whether "Restricted Data" is included. Marking is to be in accordance with appropriate security regulations.

2b. GROUP: Automatic downgrading is specified in DoD Directive 5200.10 and Armed Forces Industrial Manual. Enter the group number. Also, when applicable, show that optional markings have been used for Group 3 and Group 4 as authorized.

3. REPORT TITLE: Enter the complete report title in all capital letters. Titles in all cases should be unclassified. If a meaningful title cannot be selected without classification, show title classification in all capitals in parenthesis immediately following the title.

4. DESCRIPTIVE NOTES: If appropriate, enter the type of report, e.g., interim, progress, summary, annual, or final. Give the inclusive dates when a specific reporting period is covered.

5. AUTHOR(S): Enter the name(s) of author(s) as shown on or in the report. Enter last name, first name, middle initial. If military, show rank and branch of service. The name of the principal author is an absolute minimum requirement.

6. REPORT DATE: Enter the date of the report as day, month, year; or month, year. If more than one date appears on the report, use date of publication.

7a. TOTAL NUMBER OF PAGES: The total page count should follow normal pagination procedures, i.e., enter the number of pages containing information.

7b. NUMBER OF REFERENCES: Enter the total number of references cited in the report.

8a. CONTRACT OR GRANT NUMBER: If appropriate, enter the applicable number of the contract or grant under which the report was written.

8b, 8c, & 8d. PROJECT NUMBER: Enter the appropriate military department identification, such as project number, subproject number, system numbers, task number, etc.

9a. ORIGINATOR'S REPORT NUMBER(S): Enter the official report number by which the document will be identified and controlled by the originating activity. This number must be unique to this report.

9b. OTHER REPORT NUMBER(S): If the report has been assigned any other report numbers *(either by the originator or by the sponsor)*, also enter this number(s).

10. AVAILABILITY/LIMITATION NOTICES: Enter any limitations on further dissemination of the report, other than those imposed by security classification, using standard statements such as:

(1) "Qualified requesters may obtain copies of this report from DDC."

(2) "Foreign announcement and dissemination of this report by DDC is not authorized."

(3) "U. S. Government agencies may obtain copies of this report directly from DDC. Other qualified DDC users shall request through _____."

(4) "U. S. military agencies may obtain copies of this report directly from DDC. Other qualified users shall request through _____."

(5) "All distribution of this report is controlled. Qualified DDC users shall request through _____."

If the report has been furnished to the Office of Technical Services, Department of Commerce, for sale to the public, indicate this fact and enter the price, if known.

11. SUPPLEMENTARY NOTES: Use for additional explanatory notes.

12. SPONSORING MILITARY ACTIVITY: Enter the name of the departmental project office or laboratory sponsoring *(paying for)* the research and development. Include address.

13. ABSTRACT: Enter an abstract giving a brief and factual summary of the document indicative of the report, even though it may also appear elsewhere in the body of the technical report. If additional space is required, a continuation sheet shall be attached.

It is highly desirable that the abstract of classified reports be unclassified. Each paragraph of the abstract shall end with an indication of the military security classification of the information in the paragraph, represented as *(TS), (S), (C), or (U)*.

There is no limitation on the length of the abstract. However, the suggested length is from 150 to 225 words.

14. KEY WORDS: Key words are technically meaningful terms or short phrases that characterize a report and may be used as index entries for cataloging the report. Key words must be selected so that no security classification is required. Identifiers, such as equipment model designation, trade name, military project code name, geographic location, may be used as key words but will be followed by an indication of technical context. The assignment of links, rules, and weights is optional.

Security Classification